Functional and transcriptional profiling of non-coding RNAs in yeast reveal context-dependent phenotypes and widespread *in trans* effects on the protein regulatory network

Laura Natalia Balarezo-Cisneros[1,2], Steven Parker[1,2], Marcin G Fraczek[1,2], Soukaina Timouma[1,2], Ping Wang[2], Raymond T O'Keefe [2], Catherine B Millar [2*], Daniela Delneri [1,2*]

[1]Manchester Institute of Biotechnology, Faculty of Biology Medicine and Health, The University of Manchester, 131 Princess street, M1 7DN, UK

[2]Division of Evolution and Genomic Sciences, Faculty of Biology, Medicine and Health, The University of Manchester, Oxford Road, Manchester M13 9PL, UK

*Correspondence should be addressed to DD (d.delneri@manchester.ac.uk) or CM (catherine.millar@manchester.ac.uk).

Key words: non-coding RNA, transcriptome, yeast, transcription factors, *trans* effect, genetic interactions

Abstract

Non-coding RNAs (ncRNAs), including the more recently identified Stable Unannotated Transcripts (SUTs) and Cryptic Unstable Transcripts (CUTs), are increasingly being shown to play pivotal roles in the transcriptional and post-transcriptional regulation of genes in eukaryotes. Here, we carried out a large-scale screening of ncRNAs in *Saccharomyces cerevisiae*, and provide evidence for SUT and CUT function. Phenotypic data on 372 ncRNA deletion strains in 23 different growth conditions were collected, identifying ncRNAs responsible for significant cellular fitness changes. Transcriptome profiles were assembled for 18 haploid ncRNA deletion mutants and 2 essential ncRNA heterozygous deletants. Guided by the resulting RNA-seq data we analysed the genome-wide dysregulation of protein coding genes and non-coding transcripts. Novel functional ncRNAs, SUT125, SUT126, SUT035 and SUT532 that act *in trans* by modulating transcription factors were identified. Furthermore, we described the impact of SUTs and CUTs in modulating coding gene expression in response of different environmental conditions, regulating important biological process such as respiration (SUT125, SUT126, SUT035, SUT432), steroid biosynthesis (CUT494, SUT530, SUT468) or rRNA processing (SUT075 and snR30). Overall, this data captures and integrates the regulatory and phenotypic network of ncRNAs and protein coding genes, providing genome-wide evidence of the impact of ncRNAs on cellular homeostasis.

Author Summary

The yeast genome contains 25% of non-coding RNA molecules (ncRNAs), which do not translate into proteins but are involved in regulation of gene expression. ncRNAs can affect nearby genes by physically interfering with their transcription (*cis* mode of action), or they interact with DNA, proteins or others RNAs to regulate the expression of distant genes (*trans* mode of action). Examples of *cis*-acting ncRNAs have been broadly described, however genome-wide studies to identify functional *trans*-acting ncRNAs involved in global gene

regulation are still lacking. Here, we used the ncRNA yeast deletion collection to score their impact on cellular function in different environmental conditions. A group of 20 ncRNAs mutants with broad fitness diversity were selected to investigate their effect on the protein and ncRNA expression network. We showed a high correlation between altered phenotypes and global transcriptional changes, in an environmental dependent manner. We confirmed the widespread *trans* acting expressional regulation of ncRNAs in the genome and their role in affecting transcription factors. These findings support the notion of the involvement on ncRNAs in fine tuning the cellular expression via regulations of TFs, as an advantageous RNA-mediated mechanism that can be fast and cost-effective for the cells.

Introduction

Gene regulation is a key biological process across all life forms, and multiple gene interactions quickly allow adaptation to different conditions in response to environmental stimuli. This response may induce adaptation to various food sources, trigger alternative metabolic pathways, or overcome stress factors.

Chromatin modifications and DNA methylation are two main mechanisms of regulating gene expression. More recently, RNA transcripts which are not translated into protein, have been described to have a prominent role as epigenetic modifiers [1,2]. There are an increasing number of examples of these non-coding RNA (ncRNA) transcripts regulating gene expression positively and negatively [3-10].

RNA interference (RNAi) was the first understood example of ncRNA involvement in epigenetics [11]. This RNAi mechanism involves ncRNAs binding to target mRNA sequences, inhibiting their translation [12]. *Saccharomyces cerevisiae* (*S. cerevisiae*) lacks RNAi machinery; however, a large number of non-coding transcripts have been identified in this budding yeast using high-throughput and high-resolution technologies. These ncRNA transcripts come from what is known as “pervasive transcription”, a mechanism that generates RNAs distinct from those that encode proteins or those with established functions (*e.g.* snoRNAs, snRNAs, rRNAs) [13]. Among a list of catheterized pervasive transcripts, Stable

Unannotated Transcripts (SUTs) and Cryptic Unstable Transcripts (CUTs) show an essential role in gene regulation, influencing histone modifications or regulating transcription of nearby genes [4,5,14–16].

SUTs and CUTs are polyadenylated RNAs transcribed by RNA polymerase II [17] and are distributed across the entire *S. cerevisiae* genome. Classically, SUTs and CUTs arise from nucleosome-depleted regions (NDRs) associated with bidirectional promoters of protein-coding genes [17,18], but differ in their association with the RNA decay machinery. CUTs are capped and degraded rapidly by the nuclear exosome and the TRAMP (Trf4-Air1/Air2-Mtr4) complex [19], whereas SUTs are only partially susceptible to Rrp6p activity [17] and are mainly affected by cytoplasmic RNA decay pathways including the translation-dependent nonsense-mediated decay (NMD) pathway and Xrn1- dependent 5' to 3' degradation [20]. As a result, SUTs persist longer than CUTs.

Gene regulation activities have been ascribed to SUTs and CUTs. In many cases, ncRNAs appear to cause transcriptional interference [3,5,15,16,21-23] affecting the expression of neighbouring genes in *cis*. On the other hand, ncRNAs can be functional and regulate in *trans* the expression of genes located both nearby or at distant loci [4,6,10]. Although only a small number of functional ncRNAs have been well characterized to date, they have been shown to control gene expression at the transcriptional level. For instance, SUT075 has recently been reported to regulate the expression of *PRP3* when overexpressed remotely on a plasmid [10]. Another example is SUT457, which is involved in telomere organization. SUT457 regulates the levels of telomeric ssDNA in a Exo1-dependent manner [9]. Interestingly, CUT281, known as *PHO84* ncRNA because it overlaps the protein-coding *PHO84* gene, triggers *PHO84* silencing in a *trans* and *cis* manner using two independent mechanisms. While the *cis*-acting mechanism requires Hda1/2/3 deacetylation machinery, *trans* function is generated by the Set1 histone methyltransferase [5,6].

Emerging evidence has suggested ncRNAs roles in the recruitment of transcription factors (TFs) to their binding sites in fission yeast, mouse and humans [21-26], thus,

suggesting a conserved mechanism of gene expression among eukaryotes. On one hand, ncRNA expression around regulatory elements can locally promote TF binding [23-24]. On the other hand, ncRNA can regulate gene expression by acting as binding competitors for DNA-binding proteins (DBPs) [25-26].

Considerable progress has been made over the past decade to elucidate the unique features and molecular mechanisms of ncRNA. However, detailed insights have been limited to single ncRNA genes, usually affecting neighbouring genes. Here, we combine large-scale phenotypic analysis with RNA-seq technology to generate a global view of the transcriptome following ncRNA deletion. Specifically, by analysing the expression network, we show that the global transcriptional effect of deleting four SUTs is indirect and acts via specific TFs whose level of expression is affected by deleting these ncRNAs. This *trans* effect supports and extends previous premises that SUTs or CUTs are a functional part of the genome and can influence the general transcriptional output of a cell independent from where they are located.

Results and Discussion

Fitness profiling of haploid ncRNA deletion strains reveals plasticity of phenotype in different environmental conditions

To investigate the plasticity of ncRNA deletion mutations on organism fitness, we acquired phenotypic data for the haploid ncRNA deletion collection generated by Parker *et al.* (2017) in 23 different conditions. The ability of 50 CUT, 93 SUT, 61 snoRNA and 168 tRNA deletion mutant strains to utilize different carbon sources, and to tolerate extreme pH and oxidative stress was scored. The colony size was used as a proxy for fitness and normalized to the wild-type strain according to Tong and Boone [9]. The ncRNA deletion mutants showing similar behaviour across the 23 different conditions were grouped, generating 42 distinct functional clusters (Fig 1). The list of deletion mutant strains in each cluster is reported in the Supplementary Dataset S1.

About 45% of the ncRNA deletion mutants analysed did not show significant phenotypic changes in any condition tested, while about 24% of the ncRNA deletion strains showed significant changes in fitness in at least one condition tested. The remaining ncRNA deletion mutants (*i.e.* clusters 1 to 5) displayed a severe fitness defect in the majority of conditions, in particular when grown in ethanol, glycerol, sorbitol or melezitose as carbon sources. These clusters contained mostly tRNAs and SUTs rather than CUTs and snoRNAs (Supplementary Dataset S1). The conditions that affected the least number of ncRNA deletion mutants were YP+ 2% Fructose, YPD+ 5% Methanol, and YPD+ 5% Isopropanol, which affected 4.3%, 4.5% and 5.1% of ncRNA deletion mutants, respectively. Conditions that induced the broadest fitness changes were YP+ 7% Ethanol and YP+ 2% Glycerol, with 11.8% and 11.5% of ncRNA deletion mutants affected, respectively (Fig 1 and Supplementary Dataset S1).

Liquid growth assays were also set up for SUT and CUT deletion mutants that displayed either severe fitness defects (clusters 1, 2 and 5), fitness gain (clusters 7 to 9), or no phenotype (cluster 10). The overall liquid growth phenotype is reported as relative area under the growth curve (Fig 2), and the breakdown for the different growth phases is available in Table S1. Overall, in rich media, the majority of deletion mutant strains showed no growth difference, with the exception of the reduced fitness of *SUT125*Δ, *SUT126*Δ and CUT494/SUT053/SUT468*Δ* and the improved fitness of *CUT248Δ* (S1 Table).

When 10% ethanol was added to the media, *SUT125Δ*, *SUT126Δ*, *SUT035Δ*, *SUT532Δ*, *SUT129Δ* and *CUT494/SUT053/SUT468Δ* displayed severe fitness defects affecting the majority of the growth phases (Fig 2A and S1 Table); a similar profile for fitness impairment for SUT125, SUT126 and SUT035 was observed in media containing either 5% ethanol (Fig 2B) or 2% glycerol (Fig 2C). However, *SUT532Δ* and *SUT129Δ* had a divergent fitness profile in 5% ethanol and 2% glycerol. *SUT532Δ* presented a significant fitness defect in YP+ 5% Ethanol and a growth improvement in YP+ 2% Glycerol (Fig 2B and C), whereas *SUT129Δ* showed an improvement in YP+5% Ethanol and defect in 2% glycerol.

Several SUTs and CUTs displayed improved fitness in the YP+ 5% Ethanol liquid media (Fig 2B) revealing a similar phenotypic change in both solid and in liquid media. About 56% of the

158 strains grown in YPD+10% Ethanol and 27.7% of the strains grown in YP+ 2% Glycerol
159 displayed some differences in fitness profiles between solid and liquid media. For example,
160 *CUT494/SUT053/SUT468Δ*, *SUT129Δ*, *SUT329Δ* and *CUT442Δ* exhibited fitness impairment
161 in YP+ 2% Glycerol which was not previously detected in the solid fitness assay.
162 Discrepancies between solid and liquid fitness are likely due to the differing oxygen availability
163 and diffusion rates of one or more nutrients on solid media [27-31]. Indeed, when growing on
164 solid surfaces, colony morphology differs between yeast growth phases and time [32–34].
165 Therefore, these results re-iterate the importance of acquiring data from both solid and liquid
166 growth assays for an accurate picture of cellular fitness.

167 **ncRNA deletions drive global transcriptional changes that correlate with**
168 **phenotypic profiles**

169 The main function previously ascribed to ncRNAs in budding yeast is transcriptional
170 regulation, usually of neighbouring or overlapping single genes [3, 4, 7, 16, 35, 36] We
171 therefore investigated by RNA-seq whether selected ncRNA deletion mutants with altered
172 phenotypes also have dysregulated transcriptomes. We selected 18 haploid ncRNA deletion
173 mutants from clusters 1, 2, 5 and 7-10 with different types of phenotypic changes (*i.e*. growth
174 defects, improvements and no changes) to study by RNA-seq, together with heterozygous
175 deletions of 2 essential ncRNAs, namely SUT075 and snR30 (previously described in Parker
176 et al [10]) (Table 1). As expected, we detected changes in the levels of at least one
177 neighbouring transcript in 8 of the ncRNA deletion mutant strains analysed by RNA-seq. Three
178 of these deletion mutants (*SUT099Δ*, *SUT722Δ*, *SUT171Δ*) up-regulate only their
179 neighbouring genes, while the remainder (*CUT494/SUT053/SUT468Δ*, *SUT532Δ*, *SUT035Δ*,
180 and *SUT125Δ*) also revealed altered levels of distantly located transcripts. Strikingly, over
181 one-third of the deletion mutants studied by RNA-seq had large numbers (>100) of
182 differentially expressed (DE) coding and non-coding transcripts (Table 1).
183
184

185 **Table 1**. Numbers of protein-coding genes and non-coding transcripts that are differentially
186 expressed in 18 SUT and CUT deletants. A 'neighbour' gene or transcript is defined as an
187 adjacent genomic feature.

		Protein- coding genes				Non-coding DNA			
	SUT/CUT	**Number of DE genes**	**Up - Regulated**	**Down-Regulated**	**Neighbour DE gene**	**Number of DE transcripts**	**Up - Regulated**	**Down-Regulated**	**Neighbour DE transcript**
Cluster 1	SUT035	701	256	445	1	232	138	94	0
	SUT125	721	310	411	2	196	106	90	0
Cluster 2	SUT126	787	335	452	0	223	141	82	0
Cluster 5	SUT532	408	236	172	0	92	55	37	1
Cluster 7	CUT494/ SUT530/ SUT468	137	102	35	1	32	6	26	0
	CUT123	0	0	0	0	0	0	0	0
	CUT248	2	2	0	0	0	0	0	0
Cluster 8	SUT129	16	8	8	0	2	1	1	0
	SUT304/ SUT730	1	0	1	0	0	0	0	0
	SUT329	1	0	1	0	0	0	0	0
	SUT722	1	1	0	1	0	0	0	0
Cluster 9	SUT171	2	1	1	1	0	0	0	0
	SUT346	1	0	1	0	0	0	0	0
	SUT465	0	0	0	0	0	0	0	0
Cluster 10	CUT442	2	0	2	0	0	0	0	0
	SUT099	2	1	1	1	0	0	0	0
	SUT451	0	0	0	0	0	0	0	0
	SUT492	1	0	1	0	0	0	0	0

188

189 Half of the deletion mutant strains had smaller numbers of differentially expressed
190 transcripts, while only three deletion mutants did not lead to transcriptional changes in rich
191 medium. Overall, transcription profiles of the ncRNA deletion mutants correlated well with their
192 fitness changes. For instance, heterozygous deletions of the two essential ncRNAs SUT075
193 and snR30 have overall a stronger negative effect on strain fitness in all the conditions tested
194 (S1 Fig). As expected, these deletions affected the largest number of transcripts (Table 2).

Table 2. Differentially expressed protein-coding genes and non-coding transcripts in heterozygous deletions of the essential ncRNA genes *snR30* and *SUT075*.

	Protein-coding genes				Non-coding DNA			
	Number of DE genes	Up - Regulated	Down-Regulated	Neighbour	Number of DE transcripts	Up - Regulated	Down-Regulated	Neighbour
snR30	2276	1063	1213	0	408	335	73	2
SUT075	2284	1057	1227	1	292	238	54	0

The two apparently unrelated essential ncRNAs, SUT075 and snR30, have a surprisingly large number of DE transcripts in common (about 80%; 864 up-regulated and 972 down-regulated). Gene Ontology (GO) analysis of the shared DE protein-coding genes revealed enrichment for ribosome biogenesis, ribosomal RNA processing, DNA replication and the cell cycle (S2 Fig). This GO enrichment is consistent with the known role of snR30 in ribosomal RNA processing [37]. SUT075 is required for normal transcript levels of its neighbouring essential gene *PRP3* and can act in *trans* [10]. We note however, in our RNA-seq data, that the down-regulation of *PRP3* was not significantly strong (fold change, FC, 0.7) in *SUT075*Δ and instead a large global effect on the transcriptome was detected, including targets in common with the snR30 mutant. A further 481 essential genes are affected in addition to *PRP3* when SUT075 is deleted (82 up-regulated and 399 down-regulated) representing 43% of the *S. cerevisiae* essential genes. As a comparison, *snR30*Δ dysregulates 450 essential genes (ca. 40%), up-regulating and down-regulating 82 and 368, respectively. Nineteen small RNAs are dysregulated in *snR30*Δ, including the essential snR19 and LSR1 (U1 and U2 snRNAs) that are part of the major spliceosome in yeast, and the RNA component of nuclear RNase P (*RPR1*) and RNase MRP (*NME1*). Interestingly, 17 snoRNAs, of which 11 are in common with *snR30*Δ, are also differentially expressed in *SUT075*Δ. Our data suggest that several factors, including an effect on the neighbouring gene *PRP3* and a potential role in rRNA processing, may cause the essentiality of SUT075.

Discordant changes between transcriptome and fitness as a tool to reveal additional context-dependent phenotypes

Generally, the clusters containing ncRNA deletion mutants that do not impair fitness also do not produce significant global transcriptional changes and vice-versa. However, there was one exception to this pattern in cluster 7 that contained ncRNA deletion mutants with largely unaffected fitness except for *CUT494/SUT053/SUT468Δ*. The deletion of CUT494/SUT053/SUT468 caused the dysregulation of over 150 transcripts, in contrast to the deletion of CUT123 or CUT248, which affected 0 and 2 transcripts respectively. To investigate this apparent discrepancy, we used GO analysis to identify enriched functional categories across the 137 DE genes in *CUT494/SUT053/SUT468Δ*. The majority of the over-represented GO terms were related to the synthesis of crucial membrane components and membrane fluidity pathways. Specifically, GO biological process categories enriched among down-regulated genes included sterol, steroid, ergosterol and lipid biosynthesis, while up-regulated genes were clustered in pathways for propionate metabolism, drug response and molecular transport (S3 Fig). Ergosterol (ERG) is an essential membrane component that regulates membrane fluidity, permeability, membrane-bound enzyme activity and substance transportation [38]. Overexpression or deletion of ERG biosynthesis genes results in the accumulation of toxic intermediates, alteration of drug sensitivity and slow growth in different media, including non-fermentable carbon sources [39]. Interestingly, our fitness data revealed a growth defect of the *CUT494/SUT053/SUT468*Δ strain in YP+2% Glycerol (Fig 2C). To test the hypothesis that *CUT494/SUT053/SUT468*Δ has a role in membrane stability by targeting synthesis of ERG, we used azole antifungal agents that inhibit various steps in the ERG biosynthesis pathway [40]. When the fitness of *CUT494/SUT053/SUT468Δ* was tested in medium supplemented with either fluconazole (Fig 3A and C) or miconazole (Fig 3B and D), a slow growth phenotype was identified compared to the WT and the other deletion

mutants in the same cluster (Fig 3). This result suggests that transcriptome data can be used to identify environmental conditions that are likely to reveal fitness defects.

ncRNAs with related phenotypes regulate common genes involved in mitochondrial functions

SUTs/CUTs clustered together by their fitness profile are expected to engage similar biological and molecular functions. To test this premise, we identified the set of common DE genes across deletion mutant strains that are part of the same phenotypic cluster. Remarkably, SUT125, SUT126 and SUT035 (clusters 1 and 2) dysregulate 481 coding genes (286 downregulated and 195 up-regulated) and 126 non-coding transcripts in common (Fig 4A and B). Moreover, those ncRNA deletion mutants displayed negative fitness during phenotypic analysis when growing in 22 out of the 23 media tested. To demonstrate the accuracy of our gene expression measurements, we selected a few candidate DE genes from the deletion mutants in clusters 1 and 2, and tested their mRNA levels by RT-qPCR. Among the selected genes, down-regulated and up-regulated expression fold change by qPCR were similar to the expression fold change obtained from the RNA-Seq data (S4 Fig and S2 Dataset), validating the RNA-seq data.

To identify the biological processes associated with the commonly misregulated genes in clusters 1 and 2, the set of DE genes was analysed for GO term enrichment and the most significant hits were selected. Genes with decreased and increased expression were associated with key mitochondrial functions such as mitochondrial electron transport and oxidation-reduction process (S5 Fig). The enriched pathways identified from KEGG and Reactome data (Holm-Bonferroni correction) were branched amino acid biosynthesis (p-value 5e-4 7 matches), aerobic respiration, electron transport chain (p-value=0.002 11 matches), mevalonate pathway (p-value= 0.004 5 matches) and TCA cycle (p-value= 0.021 9 matches), also indicating roles in mitochondrial functions. When strains in cluster 5 are included along with clusters 1 and 2, there are 96 protein-coding genes (Fig 5) and 15 non-coding genes dysregulated in common (S6 Fig). Those common genes have, in general, a concordant

expression profile between each ncRNA deletion mutant strain. However, for 40% of the common genes, specifically those involved in mitochondrial function, an opposite expression trend is detected in the *SUT532*Δ strain (cluster 5) compared to *SUT125*Δ, *SUT126*Δ and *SUT035*Δ. Since the phenotypes of *SUT125*Δ, *SUT126*Δ, *SUT035*Δ and *SUT532*Δ mutants in different environmental conditions are similar; these 18 genes with different directionality of expression may either not be crucial for the observed phenotype, or specific to the mechanism of action for SUT532 in the cell (Fig 5). Due to the divergent fitness shown in glycerol for *SUT532*Δ strain we sought to elucidate if there are specific mitochondrial pathways in which SUT532 could be involved. Thus, GO of the non-common genes (321) for this ncRNA deletion mutant was also performed. Interestingly, up-regulated genes are related to the TCA cycle and aerobic respiration along with protein refolding and response to stress. Down-regulated genes are mainly involved with leucine biosynthesis biological process. (S7 Fig). Taken together, these results reveal enrichment of mitochondrial roles for SUT125, SUT126, SUT035 and SUT532 suggesting their potential function in repressing or activating mitochondrial metabolic pathways, justifying the fitness impairment of those deletion mutants when grown with non-fermentative carbon sources.

ncRNAs drive global transcriptome changes through transcription factors

The finding that large numbers of genes involved in the same pathways are DE in ncRNA deletion mutant strains led us to hypothesize that these ncRNAs may be acting via sequence-specific transcription factors (TFs) that regulate these groups of genes. Using the YEASTRACT database [41–44], we identified TFs that are up- or down-regulated in *SUT125*Δ, *SUT126*Δ, *SUT035*Δ, *SUT532*Δ and *CUT494/SUT053/SUT468*Δ mutants, which all show large transcriptional changes. We found that several TFs were significantly perturbed in *SUT125*Δ, *SUT126*Δ, *SUT035*Δ, *SUT532*Δ and *CUT494/SUT053/SUT468*Δ, affecting ca 16%, 19%, 20%, 13% and 5% of all annotated yeast TFs (ca. 183), respectively. The number of TFs with altered expression is significant in *CUT494/SUT530/SUT468*Δ, *SUT126*Δ,

297 *SUT035*Δ, and *SUT532*Δ with p-values lower than 0.05 upon chi-square test (S2 Table).
298 Several DE TFs, such as *PDR3*, *MOT3* and *YOX1*, were shared among *SUT125*Δ, *SUT126*Δ,
299 *SUT035*Δ (S8 Fig). The expression changes for these three TFs were validated with *SUT126*Δ
300 via real time PCR (S5 Fig), showing a strong agreement between the qPCR and RNA seq
301 data.

302 As the most significant fitness phenotypes observed for ncRNA deletion mutant strains
303 were in YP or YPD media supplemented with ethanol, we identified those TFs whose mis-
304 regulation has been linked to ethanol resistance. Many ethanol-tolerance genes share a TF-
305 binding motif recognized by Pdr1 and Pdr3 [45]. In the *S. cerevisiae* genome, 12.39% of genes
306 are Pdr3 targets [44]. Strikingly, about 95% ($p < 0.0001$) of DE genes in *SUT126*Δ, *SUT125*Δ
307 and *SUT035*Δ are targets of this zinc finger protein that acts predominantly as a transcriptional
308 activator [44, 47, 48] and whose transcript levels significantly increase in the same ncRNA
309 deletion mutant strains (S2 Dataset and S5E Fig). Furthermore, *MNS4,* which encodes a key
310 regulator for ethanol tolerance [45,48], is up-regulated when SUT532 is deleted and down-
311 regulated when SUT035 is deleted (S2 Dataset). Accordingly, 40.4% of dysregulated genes
312 in the *SUT532Δ* and 37.7% in *SUT035Δ* are targets of Msn4. These data suggest that
313 SUT125, SUT126, SUT035 and SUT532 ncRNAs are associated with mechanisms of ethanol
314 tolerance that may involve a massive gene expression reprogramming resulting from the shift
315 from fermentative to non-fermentative metabolism. Moreover, they imply that ncRNAs may be
316 part of the activation or repression of metabolic pathways and regulatory networks through
317 modulation of TFs.

318 To test whether the upregulation of Pdr3 target genes upon ncRNA deletion is Pdr3-
319 dependent, we investigated the expression of previously validated Pdr3p target genes [46,
320 50–53] in the *SUT126Δ* background. We found that the SUT126 deletion is not sufficient to
321 activate Pdr3 target genes *ACO1*, *BDH2* or *RSB1* in the absence of Pdr3 (Fig 6). These results
322 suggest that the global effect on the transcriptome observed in the absence of SUT126 is
323 likely driven by an effect of this ncRNA on TFs such as Pdr3. SUT126 may have a repressive

effect on the promoter of *PDR3,* may destabilize the *PDR3* transcript, or, as *PDR3* is autoregulated, may bind to and interfere with the Pdr3 protein. Several ncRNAs have been reported to bind transcription factors to regulate gene expression in other organisms. For example, in mice, the long-ncRNA (lncRNA) *linc-YY1,* involved in myogenesis, has been found to interact with the TF *YY1* [24]. Similarly, *GAS5* interacts with glucocorticoid receptors, supressing their binding with glucorticoid response elements [26]. In humans, lncRNA rhabdomyosarcoma 2–associated transcript (RMST) interacts directly with Sox2, a transcription factor involved in the regulation of embryonic development [54]. Regulation of gene expression by ncRNAs acting through transcription factors might, therefore, be a conserved mechanism among eukaryotes. In this way ncRNAs could confer an extra advantage to yeast cells by modulating gene expression in response to environmental stress.

Phenotypic and transcriptional effects of the *KanMX* cassette used to generate ncRNA deletions on neighbouring genes

The *kanMX* cassette used to make the ncRNA deletion mutant strains has been suggested to affect the expression of neighbouring genes, either because of its high transcriptional level or via the generation of unexpected antisense transcripts [55–58]. We did not observe any alteration in transcript levels of neighbouring genes in the majority (13/20) of the ncRNA deletion mutant strains that we studied (Table 1) but levels of one or both neighbouring transcripts were affected in the remainder and might, therefore, contribute to the observed changes in phenotype and gene expression. For example, *SUT125Δ*, besides globally affecting the transcriptome, also has an effect on both of its neighbouring genes, *PIL1* and *PDC6*. Levels of *PIL1 mRNA* are reduced while *PDC6* transcript levels are higher in the mutant.(S3 Fig and S2 Dataset) To test whether *kanMX* cassette insertion replacing SUT125 causes the local expression changes , the mRNA levels of *PDC6* and *PIL1* were quantified and compared in three different SUT125 deletion mutant strains containing: *i.* the *kanMX* cassette in sense orientation relative to *SUT125*; *ii.* the *kanMX* cassette in antisense

orientation relative to *SUT125*; *iii*. a *loxP* scar after *kanMX* excision with the Cre/loxP system (i.e. no *kanMX* cassette). The down-regulation of the expression of *PIL1* remains the same in all three mutants, ruling out a transcriptional effect of the *kanMX* cassette on *PIL1* expression (Fig 7A). *PDC6* is up-regulated in all three mutants, however the effect is stronger when the *kanMX* cassette is removed (Fig 7B). This result suggests a partial effect of the *kanMX* on *PDC6* expression, where the presence of the cassette either in sense or antisense orientation dampens the up-regulatory effect.

To identify whether *PIL1* down-regulation and *PDC6* overexpression trigger the growth changes observed in *SUT125Δ* in medium containing ethanol we carried out spot test growth assays. *PDC6* was overexpressed from a plasmid to mimic up-regulation, and a *PIL1* deletion strain was used to mimic *PIL1* downregulation. The combined effect was scored in a *PIL1Δ* strain harbouring the *PDC6* overexpression plasmid. Presence or absence of *the kanMX* cassette reveals little to no effect on the resulting phenotype (Fig 8). Overexpression of *PDC6* in a WT background produced the same phenotype as a SUT125 deletion, while either *PIL1Δ* or *PDC6Δ* deletion did not have any effect on the phenotype (Fig 8). The concomitant effect of over-expressing of *PDC6* in *PIL1Δ* strain produced a less severe, but still comparable, phenotype to that of a SUT125 deletion. These data suggest that *PDC6* overexpression alone may account for the majority of the phenotype following *SUT125Δ* deletion.

The effect of the *kanMX* cassette on growth phenotypes was also tested in *SUT126Δ*, which has a fitness impairment, and SUT129Δ, which displays a fitness gain. Similar fitness profiles were observed regardless of the presence or absence of *kanMX* for all the ncRNA mutants (Fig 9). In addition, the effect of the *kanMX* selectable marker on transcription of non-neighbouring DE genes was tested by quantifying and comparing the mRNA levels of Pdr3p and Yox1p transcription factors in *SUT126* and *SUT125* deletion mutant strains with and without *kanMX*. No significant differences in the expression levels of *YOX1 and PDR3* were detected (S9 Fig). In summary, these data indicate that phenotypic and transcriptional changes observed in these ncRNA deletion mutants are not dependent on the presence of an actively transcribed drug resistance marker gene. Moreover, the majority of the ncRNA

379 deletion mutants tested do not have any effect on transcript levels of neighbouring genes,
380 suggesting a genuine effect on distant genetic loci in *trans*.

381 **ncRNAs SUT125, SUT126, SUT035 and SUT532 act in *trans* to regulate target**
382 **genes**

383 The deletion of SUT126, SUT125, SUT035 or SUT035 led to widespread changes in
384 the global transcription network (S2 Dataset). These ncRNAs may therefore function in *trans*
385 by affecting distant genes. To test this hypothesis, ectopically expressed SUT125, SUT126,
386 SUT035 and SUT532 were assessed for their ability to rescue growth defects in the presence
387 of 5% ethanol. Each of these SUTs was placed under control of an inducible *GAL1* promoter
388 on a plasmid that was transformed into the respective deletion mutant. Under conditions where
389 the *GAL1* promoter is repressed (glucose) there ware no differences in growth between
390 deletion strains carrying the *GAL1-SUT* plasmid or an empty version of this plasmid. However,
391 when *GAL1*-driven expression was induced (galactose), all four SUTs were able to rescue the
392 growth defect (Fig 10). These results suggest that SUT126, SUT126, SUT035 and SUT532
393 can act *in trans*, which may underlie the altered regulation of large numbers of genes in these
394 mutants. There are only a handful of examples of *trans* acting ncRNAs in yeast but a CUT that
395 affects gene regulation, CUT281, can act both in *cis* and *trans* to repress the *PHO84* gene [6,
396 36], while SUT457 can act in *trans* to rescue the phenotype of telomeric overhang
397 accumulation observed in *SUT457Δ* cells [9].

398 ## Conclusion

399 Large-scale phenotypic projects using deletion mutant collections have proven to be
400 an invaluable tool for linking genes to their function [59–62]. Here we used 372 haploid strains
401 from the ncRNA deletion collection [10] to identify deletions that are responsible for phenotypic
402 changes in 23 environmental conditions. The fitness data obtained has been integrated into
403 the Yeast ncRNA Analysis (YNCA) database (http://sgjlab.org:3838/ynca/) [10]. Based on the
404 phenotypic screening data, we further analysed 20 ncRNA deletion mutants at the

transcriptome level. ncRNA deletion mutants that were phenotypically impaired also triggered significant changes in the gene regulatory network. By analysing the expression data, we identified specific pathways where these SUTs and CUTs were functioning, such as mitochondrial function and respiration, ethanol tolerance, rRNA processing, plasma-membrane fluidity and sterol biosynthesis. In the *SUT126*Δ strain, we showed that the large transcriptional changes are due to the altered expression of TFs rather than the direct effect of the lncRNA deletion. These results indicate that ncRNAs are likely to be involved in fine tuning expression by regulating the expression of TFs.

Gene regulation driven by ncRNAs through TFs may be a conserved mechanism amongst eukaryotes. Examples of ncRNAs enhancing the loading of TFs at their target promoters or acting as a binding competitors for DNA/RNA binding proteins in fission yeast, mouse and human cells are increasing [23–26]. In fact, most ncRNAs are transcribed near regulatory units for transcription such as promoters or enhancers [17, 18, 63], which may be an indication that associates them with biological function and mechanism.

We discovered that SUT125, SUT126, SUT532 and SUT035 act in *trans* since their functions can be rescued ectopically. Strikingly, these ncRNAs originate from intergenic regions that do not overlap with any open reading frame, bearing out the possibility that their functionality may be linked with their potential to form accessible structural domains able to bind to DNA, RNA or proteins [64–66]

Such ncRNA mediated regulation is cost-effective compared to the classical regulation via TFs as the fast production of RNAs compared to proteins facilitates quick genetic responses to environmental stimuli.

Materials and methods

Yeast strains, growth conditions and plasmids

A list of *Saccharomyces cerevisiae* strains and plasmids is provided in S3 Table. For strain maintenance and construction, strains were grown at 30°C under standard conditions.

ncRNA single deletion strains used this study were taken from the ncRNA deletion collection created by Parker, et al [10,67]. Deletion mutants were maintained on Yeast extract Peptone Dextrose Agar (YPDA) containing 200 µg/mL G418. Double deletion mutant strains were constructed by substituting the candidate *SUT* locus with the *natNT2* cassette and were maintained on YPDA containing 100 µg/mL clonNAT.

For construction of strains ectopically expressing particular SUTs, isogenic wild-type and ncRNA deletion mutant strains cells were transformed with pRS416-Gal1-Cyc1 overexpression plasmid containing the ncRNA of interest. Resulting strains were maintained in a synthetic minimal media lacking uracil (SD-Ura: 1X Yeast Nitrogen Base (YNB) (Formedium); 1X Complete Supplement Mixture (CSM) – Ura (Formedium); 2% (w/v) glucose). For phenotypic rescue studies, strains were grown to an optical density at 600 nm (OD_{600}) of 0.5 in YP (1% yeast extract, 2% peptone) medium supplemented with 2% raffinose (YPRaf) at 30°C and induced with YP medium containing 2% galactose (YPGal) for 2 hours before being harvested for spot test assays.

Cre recombinase-mediated marker excision in *Saccharomyces cerevisiae*

SUT deletion strains containing loxP sites flanking the *kanMx* cassette were transformed with pSH-ble^r plasmid DNA, and grown on YPDA containing 10 µg/mL phleomycin. To excise the cassette, cells harboring pSH-ble^r were grown overnight in YPRaf medium, re-suspended in 10 ml YPGal medium to an OD600 of 0.3 and incubated at 30°C for 3 h. The culture was diluted and plated out on YPDA. The resulting colonies were replica-plated on YPDA containing 200 µg/mL G418 to confirm the marker loss and YPDA with 10 µg/mL phleomycin to confirm the plasmid loss. The marker loss was also verified by colony PCR.

Phenotypic analysis on solid and liquid media

Two biological and four technical replicates of the haploid deletion mutant strains were arrayed in 384 well microtitre plates. Using a Singer Rotor HDA, the 384 well cell cultures were

457 stamped onto YPDA plates and replica plated onto 23 different environmental conditions and
458 incubated at a particular temperature. A full list of the media and temperatures used in this
459 study are listed in S5 Table. Plates were imaged at 24, 48 and 72 hours using a Bio-Rad Gel
460 Doc XR system and images were processed using SGAtools [68]. The average pixel count for
461 the replicates of each strain were then normalized to the appropriate plate wild-type value then
462 mean, standard deviation and p-values were calculated assuming a normal distribution of
463 values. Strains with similar growth in different media were grouped into specific clusters.
464 For liquid fitness assays, cells were grown at 30°C from an OD_{600} nm of 0.1, and growth
465 measurements at OD595nm were recorded using a BMG FLUOstar OPTIMA Microplate
466 Reader. The readings were taken every 5 minutes as previously described by Naseeb and
467 Delneri [69] for up to 55 hours incubation time. Three technical replicates of three independent
468 biological samples were used for each deletion mutant and wild-type strain. Graphs and
469 growth parameters were produced using the *grofit* package of the *R* program.
470 For spot test assays, cultures were grown overnight before being serially diluted 1:10
471 and spotted onto agar plates.

472 **Total RNA extraction and quantitative RT-PCR**

473 Total RNA was isolated from $1x10^7$ cells using the RNeasy Mini Kit (QIAGEN,
474 Germany) following the protocol for enzymatic digestion of cell wall followed by lysis of
475 spheroplasts. To eliminate genomic DNA contamination, an additional DNAse treatment was
476 performed with RNAse-free DNase set (QIAGEN, Germany) following the manufacturer's
477 protocol. The RNA extracted was quantified using a NanoDrop LiTE Spectrophotometer
478 (THERMO SCIENTIFIC, United States). Two micrograms of total RNA were reverse
479 transcribed into cDNA using SuperScript III Reverse Transcriptase (Invitrogen, UK) according
480 to the manufacturer's protocol. Optimized qPCR reactions contained 2ng/µl of cDNA, 3pmol
481 each primer and 5 µl of iTAq Universal SYBR Green super Mix 2X in a final volume of 10 µl.
482 Reactions were cycled on a Roche Light Cycler real time System for 35 cycles of: 15 seconds
483 at 95˚C; 30 seconds at 57˚C ;and 30 seconds at 72˚C. Three biological replicates and three

technical replicates per sample were used in each experiment, and all runs included a no template control, and a control lacking reverse transcriptase. The relative expression of each gene was estimated using the Ct values relative to those of *ACT1*. Primers were designed to produce an amplicon of 80-150bp (Sequences given in S4 Table).

Illumina HiSeq library preparation and sequencing

Libraries were prepared from total RNA using the TruSeq Stranded mRNA Library Prep Kit (Illumina,Inc) according to the manufacturer's instructions. Sequencing was performed on an Illumina HiSeq4000 instrument. Sequences corresponding to protein-coding genes were mapped to sacCer3, while CUT and SUT sequences were mapped using the genomic coordiates provided by Xu et al [17]. Mapping was performed using STAR [70]. Differential gene expression analysis was based on the negative binomial distribution (DESeq2) [71]. Genes with a statistically significant difference in expression from wild-type, as indicated by a q-value below 0.1, and greater than 1.5 fold change in expression, were included in the final list of differentially expressed genes.

Bioinfomatic and statistical analyses.

Differentially expressed genes were listed and grouped as up- or down-regulated. Enriched GO terms and pathways were identified using YeastMine, with the Helmed- Bonferroni correction used to calculate adjusted *p*-values [72]. The Yeast Search for Transcriptional Regulators And Consensus Tracking (YEASTRACT) [44] database was used to look for transcription factors and their target genes.

Statistical tests were performed using Welch two sample t-test and multiple comparisons were analysed using ANOVA followed by Dunnett's test. Error bars denote standard deviations except where noted and *p*-values are indicated on Figs as: *.* p < 0.05 ** p < 0.01 ***p < 0.001 ****p <0.0001;* ns = no significant change.

Fig Legends

Fig 1. **ncRNA deletion strain fitness profiles on solid media in different environments.** Heat-map of the 42 clusters containing 372 haploid ncRNA deletion strains. Rows represent the different growth conditions and columns represent the clusters. Colour bars represent the colony size normalized to the wild-type strain which is given the arbitrary growth value of 1. Fitness reduction is represented as shades of red. Fitness increased is represented as shades of green. No fitness change is represented as yellow. Missing data is represented as white. The list of deletion mutant strains in each cluster can be found in Supporting information S1 Dataset.

Fig 1. Liquid growth assays for SUT and CUT deletants with pronounced growth differences on solid media. Bar charts show the relative area under the curve for haploid SUT and CUT deletion strains grown in (A) YPD+10% Ethanol (B) YP+ 5% Ethanol and (C) YP+2% Glycerol. The data are presented as means calculated from three biological replicates normalized to WT. Comparisons between wild-type and mutants were analysed using ANOVA followed by Dunnett's test.

Fig 3. Liquid growth assays of ncRNA deletion mutants in the presence of azoles. Growth curves of *CUT123Δ, CUT248Δ, CUT494/SUT530/SUT468Δ* and WT strains in YPD media supplemented with (A) Fluconazole (10 mg/µl) and **(**B) Miconazole (1 µM)**.** Bar charts show the mean specific growth rate (µ) of WT and ncRNA deletion strains in the presence of (C) fluconazole (10 mg/µl) and D) miconazole (1 µM). Significance of differences was assessed by *t*- tests.

Fig 4. Deletion mutant strains displaying identical fitness profiles share a significant number of differentially expressed coding and non-coding transcripts. Area proportional Venn diagrams displaying the number of differentially expressed (A) Protein-coding genes (p-

value= 2.04e-60 and (B) Non-coding transcripts (p-value=2.11e-18) in common between *SUT125Δ, SUT035Δ* and *SUT126Δ*. Venn diagrams were generated with BioVenn [73].

Fig 5. Heat map of differentially expressed genes in common between ncRNA deletion mutants with similar fitness profiles. Heat map was constructed with 96 common DE genes between *sut125Δ, SUT126Δ, SUT035Δ* and *SUT532Δ*. Colours represent the change in expression of genes, as indicated in the key on the right. DE genes in *SUT532Δ* with different transcriptional directionality from the other three ncRNA deletants are boxed.

Fig 6. Indirect gene expression changes may be driven by SUT126 ncRNA acting through transcription factors. Relative mRNA levels of A) *ACO*1, B) *BDH2,* and C) *RSB1* analysed by RT-qPCR with *SUT126Δ/PDR3Δ* single and double mutants. The increased levels of *PDR3* targets in the *SUT126Δ* single mutant are dependent on Pdr3 (*t*-test).

Fig 7. Actively transcribed *kanMX* partially decreases the regulatory effect of neighbouring genes in *SUT125* deletion strains. Transcriptional changes of SUT125 neighbouring genes (A) *PIL1* and (B) *PDC6* in *SUT125*Δ mutant strains with sense, antisense orientations (relative to SUT125) of the *kanMX* cassette, and without *kanMX* after excision with the Cre/loxP system. Relative mRNA levels were quantified by qPCR and compared by *t*-test.

Fig 8. *PDC6* overexpression may explain the majority of the *SUT125Δ* phenotype. Spot test assay of: *SUT125Δ* deletion strains with and without *kanMX; PIL1Δ* deletion strain; *PDC6* overexpression strain; and *PIL1Δ* with *PDC6* overexpression plasmid plated on (A) Synthetic minimal medium lacking uracil (SD-Ura) and (B) SD-Ura + 5% ethanol, containing either 2% glucose or 2% galactose as indicated below each panel. The *PDC6* overexpression plasmid has the *PDC6* gene under control of the inducible *GAL1* promoter in the pRS416 plasmid.

Wild-type and deletion strains containing the pRS416Gal1Cyc1 (empty plasmid) and the *PDC6Δ* deletion strain were included as controls.

Fig 9. Presence or absence of *the kanMX* cassette does not affect growth phenotypes in ncRNA deletion strains. Spot test assay of: BY4741 (WT), *SUT126Δ* and *SUT129Δ* with and without *kanMX* on (A) YPD; (B) YP+ 2% Glycerol; and (C) YP+ 5% Ethanol.

Fig 10. SUTs whose deletion results in wide-spread transcriptional changes can rescue growth phenotypes in *trans*.
Rescue spot test analysis of growth phenotypes of ncRNA deletion mutant strains containing the indicated SUT under control of the *GAL1* promoter, spotted onto SD + 5% ethanol, containing either 2% glucose (A) or 2% galactose (B). +: pRS416 with the respective SUT; - : empty plasmid.

Author Contributions: DD, CBM and ROK conceived the study; DD, CBM and LNB designed the experiments; LNB, SP and MF performed the experiments, PW and ST contributed to the initial assembly and normalisaiton of RNAseq data; LNB, CBM and DD analysed data; LNB, CBM and DD wrote the paper with the input of SP and ROK.

Acknowledgements

We thank the Genomic Technologies and Bioinformatics Facilities in the Faculty of Biology, Medicine and Health for their contribution in the acquisition and mapping of RNA-Seq data.

References

1. Peschansky VJ, Wahlestedt C. Non-coding RNAs as direct and indirect modulators of

588 epigenetic regulation. Epigenetics. 2014 Jan;9(1):3–12.

589 2. Rando OJ, Winston F. Chromatin and transcription in yeast. Genetics. 2012
590 Feb;190(2):351–87.

591 3. Martens JA, Laprade L, Winston F. Intergenic transcription is required to repress the
592 *Saccharomyces cerevisiae SER3* gene. Nature. 2004;429(6991):571–4.

593 4. Houseley J, Rubbi L, Grunstein M, Tollervey D, Vogelauer M. A ncRNA modulates
594 histone modification and mRNA induction in the yeast GAL gene cluster. Mol Cell.
595 2008;32(5):685–95.

596 5. Camblong J, Iglesias N, Fickentscher C, Dieppois G, Stutz F. Antisense RNA
597 stabilization induces transcriptional gene silencing via histone deacetylation in *S.*
598 *cerevisiae*. Cell. 2007;131(4):706–17.

599 6. Camblong J, Beyrouthy N, Guffanti E, Schlaepfer G, Steinmetz LM, Stutz F. *Trans*-
600 acting antisense RNAs mediate transcriptional gene cosuppression in *S. cerevisiae*.
601 Genes Dev. 2009 Jul 1;23(13):1534.

602 7. Hongay CF, Grisafi PL, Galitski T, Fink GR. Antisense Transcription Controls Cell Fate
603 in *Saccharomyces cerevisiae*. Cell. 2006;127(4):735–45.

604 8. Luke B, Panza A, Redon S, Iglesias N, Li Z, Lingner J. The Rat1p 5' to 3' exonuclease
605 degrades telomeric repeat-containing RNA and promotes telomere elongation in
606 Saccharomyces cerevisiae. Mol Cell. 2008;32(4):465–77.

607 9. Kyriakou D, Stavrou E, Demosthenous P, Angelidou G, San Luis B-J, Boone C, et al.
608 Functional characterisation of long intergenic non-coding RNAs through genetic
609 interaction profiling in *Saccharomyces cerevisiae*. BMC Biol. 2016;14(1):106.

610 10. Parker S, Fraczek MG, Wu J, Shamsah S, Manousaki A, Dungrattanalert K, et al. Large-
611 scale profiling of noncoding RNA function in yeast. PLOS Genet. 2018;14(3):e1007253.

612 11. Fire A, Xu S, Montgomery MK, Kostas SA, Driver SE, Mello CC. Potent and specific
613 genetic interference by double-stranded RNA in *Caenorhabditis elegans*. Nature.
614 1998;391(6669):806–11.

615 12. Fatica A, Bozzoni I. Long non-coding RNAs: new players in cell differentiation and

development. Nat Rev Genet. 2014;15(1):7–21.

13. Jensen TH, Jacquier A, Libri D. Dealing with Pervasive Transcription. Mol Cell. 2013;52(4):473–84.

14. Wu J, Delneri D, O'Keefe RT. Non-coding RNAs in *Saccharomyces cerevisiae*: what is the function? Biochem Soc Trans. 2012;40(4):907–11.

15. Thebault P, Boutin G, Bhat W, Rufiange A, Martens J, Nourani A. Transcription regulation by the noncoding RNA SRG1 requires Spt2-dependent chromatin deposition in the wake of RNA polymerase II. Mol Cell Biol. 2011;31(6):1288–300.

16. van Werven FJ, Neuert G, Hendrick N, Lardenois A, Buratowski S, van Oudenaarden A, et al. Transcription of Two Long Noncoding RNAs Mediates Mating-Type Control of Gametogenesis in Budding Yeast. Cell. 2012;150(6):1170–81.

17. Xu Z, Wei W, Gagneur J, Perocchi F, Clauder-Münster S, Camblong J, et al. Bidirectional promoters generate pervasive transcription in yeast. Nature. 2009;457(7232):1033–7.

18. Neil H, Malabat C, d'Aubenton-Carafa Y, Xu Z, Steinmetz LM, Jacquier A. Widespread bidirectional promoters are the major source of cryptic transcripts in yeast. Nature. 2009;457(7232):1038–42.

19. Wyers F, Rougemaille M, Badis G, Rousselle J-C, Dufour M-E, Boulay J, et al. Cryptic Pol II Transcripts Are Degraded by a Nuclear Quality Control Pathway Involving a New Poly(A) Polymerase. Cell. 2005;121(5):725–37.

20. Marquardt S, Hazelbaker DZ, Buratowski S. Distinct RNA degradation pathways and 3' extensions of yeast non-coding RNA species. Transcription. 2011;2(3):145–54.

21. Kornienko AE, Guenzl PM, Barlow DP, Pauler FM. Gene regulation by the act of long non-coding RNA transcription. BMC Biol. 2013 May 30;11(1):59.

22. Marchese FP, Raimondi I, Huarte M. The multidimensional mechanisms of long noncoding RNA function. Genome Biol. 2017;18(1):206.

23. Hirota K, Miyoshi T, Kugou K, Hoffman CS, Shibata T, Ohta K. Stepwise chromatin remodelling by a cascade of transcription initiation of non-coding RNAs. Nature.

644 2008;456(7218):130–4.
645 24. Sigova AA, Abraham BJ, Ji X, Molinie B, Hannett NM, Guo YE, et al. Transcription
646 factor trapping by RNA in gene regulatory elements. Science. 2015;350(6263):978–81.
647 25. Riley KJ-L, Maher LJ, III. p53 RNA interactions: new clues in an old mystery. RNA.
648 2007;13(11):1825–33.
649 26. Kino T, Hurt DE, Ichijo T, Nader N, Chrousos GP. Noncoding RNA gas5 is a growth
650 arrest- and starvation-associated repressor of the glucocorticoid receptor. Sci Signal.
651 2010;3(107):ra8.
652 27. Kamath RS, Bungay HR. Growth of yeast colonies on solid media. J Gen Microbiol.
653 1988;134(11):3061–9.
654 28. Lewis MWA, Wimpenny JWT. The influence of nutrition and temperature on the growth
655 of colonies of Escherichia coli K12. Can J Microbiol. 1981;27(7):679–84.
656 29. Barton DBH, Georghiou D, Dave N, Alghamdi M, Walsh TA, Louis EJ, et al. PHENOS:
657 a high-throughput and flexible tool for microorganism growth phenotyping on solid
658 media. BMC Microbiol. 2018;18(1):9.
659 30. Dagher SF, Ragout AL, Siñeriz F, Bruno-Bárcena JM. Cell immobilization for production
660 of lactic acid biofilms do it naturally. Adv Applied Microbiol. 2010; 71:113–148.
661 31. Rieck VT, Palumbo SA, Witter LD. Glucose availability and the growth rate of colonies
662 of Pseudomonas fluorescens. J Gen Microbiol. 1973;74(1):1–8.
663 32. Jones JC, Gray BF. Surface colony growth in a controlled nutrient environment.
664 Dependence of growth constant on nutrient concentration. Microbios. 1978;23(91):45–
665 51.
666 33. Gray BF, Kirwan NA. Growth rates of yeast colonies on solid media. Biophys Chem.
667 1974;1(3):204–13.
668 34. Cooper AL, Dean AC, Hinshelwood C. Factors affecting the growth of bacterial colonies
669 on agar plates. Proc R Soc London Ser B Biol Sci. 1968;171(23):175–99.
670 35. Bumgarner SL, Dowell RD, Grisafi P, Gifford DK, Fink GR. Toggle involving cis-
671 interfering noncoding RNAs controls variegated gene expression in yeast. Proc Natl

672 Acad Sci. 2009;106(43):18321–6.
673 36. Camblong J, Iglesias N, Fickentscher C, Dieppois G, Stutz F. Antisense RNA
674 stabilization induces transcriptional gene silencing via histone deacetylation in *S.*
675 *cerevisiae*. Cell. 2007;131(4):706–17.
676 37. Piekna-Przybylska D, Decatur WA, Fournier MJ. New bioinformatic tools for analysis of
677 nucleotide modifications in eukaryotic rRNA. RNA. 2007;13(3):305.
678 38. Hu Z, He B, Ma L, Sun Y, Niu Y, Zeng B. Recent Advances in Ergosterol Biosynthesis
679 and Regulation Mechanisms in *Saccharomyces cerevisiae.* Indian Journal of
680 Microbiology. Springer India; 2017;57:270–7.
681 39. Bhattacharya S, Esquivel BD, White TC. Overexpression or deletion of ergosterol
682 biosynthesis genes alters doubling time, response to stress agents, and drug
683 susceptibility in Saccharomyces cerevisiae. MBio. 2018;9(4).
684 40. Gebre AA, Okada H, Kim C, Kubo K, Ohnuki S, Ohya Y. Profiling of the effects of
685 antifungal agents on yeast cells based on morphometric analysis. Nielsen J, editor.
686 FEMS Yeast Res. 2015;15(5):fov040.
687 41. Abdulrehman D, Monteiro PT, Teixeira MC, Mira NP, Lourenco AB, dos Santos SC, et
688 al. YEASTRACT: providing a programmatic access to curated transcriptional regulatory
689 associations in *Saccharomyces cerevisiae* through a web services interface. Nucleic
690 Acids Res. 2011;39:D136–40.
691 42. Teixeira MC, Monteiro P, Jain P, Tenreiro S, Fernandes AR, Mira NP, et al. The
692 YEASTRACT database: a tool for the analysis of transcription regulatory associations
693 in *Saccharomyces cerevisiae*. Nucleic Acids Res. 2006;34(90001):D446–51.
694 43. Teixeira MC, Monteiro PT, Guerreiro JF, Gonçalves JP, Mira NP, dos Santos SC, et al.
695 The YEASTRACT database: an upgraded information system for the analysis of gene
696 and genomic transcription regulation in *Saccharomyces cerevisiae*. Nucleic Acids Res.
697 2014;42(D1):D161–6.
698 44. Teixeira MC, Monteiro PT, Palma M, Costa C, Godinho CP, Pais P, et al. YEASTRACT:
699 an upgraded database for the analysis of transcription regulatory networks in

Saccharomyces cerevisiae. Nucleic Acids Res. 2018;46(D1):D348–53.

45. Ma M, Liu ZL. Mechanisms of ethanol tolerance in Saccharomyces cerevisiae. Appl Microbiol Biotechnol. 2010;87(3):829–45.

46. Devaux F, Carvajal E, Moye-Rowley S, Jacq C. Genome-wide studies on the nuclear PDR3-controlled response to mitochondrial dysfunction in yeast. FEBS Lett. 2002;515(1–3):25–8.

47. Nishida-Aoki N, Mori H, Kuroda K, Ueda M. Activation of the mitochondrial signaling pathway in response to organic solvent stress in yeast. Curr Genet. 2015;61(2):153–64.

48. del Castillo Agudo L. Lipid content of *Saccharomyces cerevisiae* strains with different degrees of ethanol tolerance. Appl Microbiol Biotechnol. 1992;37(5):647–51.

49. Ma M, Liu LZ. Quantitative transcription dynamic analysis reveals candidate genes and key regulators for ethanol tolerance in *Saccharomyces cerevisiae*. BMC Microbiol. 2010;10:169.

50. Banerjee D, Lelandais G, Shukla S, Mukhopadhyay G, Jacq C, Devaux F, et al. Responses of pathogenic and nonpathogenic yeast species to steroids reveal the functioning and evolution of multidrug resistance transcriptional networks. Eukaryot Cell. 2008;7(1):68–77.

51. Salin H, Fardeau V, Piccini E, Lelandais G, Tanty V, Lemoine S, et al. Structure and properties of transcriptional networks driving selenite stress response in yeasts. BMC Genomics. 2008;9:333.

52. Schüller C, Mamnun YM, Wolfger H, Rockwell N, Thorner J, Kuchler K. Membrane-active compounds activate the transcription factors Pdr1 and Pdr3 connecting pleiotropic drug resistance and membrane lipid homeostasis in *Saccharomyces cerevisiae*. Mol Biol Cell. 2007;18(12):4932–44.

53. Weidberg H, Amon A. MitoCPR—A surveillance pathway that protects mitochondria in response to protein import stress. Science (80-). 2018;360(6385).

54. Ng SY, Bogu GK, Soh BS, Stanton LW. The long noncoding RNA RMST interacts with

728 SOX2 to regulate neurogenesis. Mol Cell. 2013;51(3):349–59.

729 55. Nguyen T, Fischl H, Howe FS, Woloszczuk R, Barros AS, Xu Z, et al. Transcription
730 mediated insulation and interference direct gene cluster expression switches. Elife.
731 2014;3:1–21.

732 56. Elison GL, Xue Y, Song R, Acar M. Insights into Bidirectional Gene Expression Control
733 Using the Canonical GAL1/GAL10 Promoter. Cell Rep. 2018;25(3):737-748.e4.

734 57. Pelechano V, Wei W, Steinmetz LM. Extensive transcriptional heterogeneity revealed
735 by isoform profiling. Nature. 2013;497(7447):127–31.

736 58. Chen M, Licon K, Otsuka R, Pillus L, Ideker T. Decoupling Epigenetic and Genetic
737 Effects through Systematic Analysis of Gene Position. Cell Rep. 2013;3(1):128–37.

738 59. Giaever G, Chu AM, Ni L, Connelly C, Riles L, Véronneau S, et al. Functional profiling
739 of the *Saccharomyces cerevisiae* genome. Nature. 2002;418(6896):387–91.

740 60. Bader GD, Heilbut A, Andrews B, Tyers M, Hughes T, Boone C. Functional genomics
741 and proteomics: charting a multidimensional map of the yeast cell. Trends Cell Biol.
742 2003;13(7):344–56.

743 61. Winzeler EA, Shoemaker DD, Astromoff A, Liang H, Anderson K, Andre B, et al.
744 Functional Characterization of the *S. cerevisiae* Genome by Gene Deletion and Parallel
745 Analysis. Science. 1999;285(5429):901–906.

746 62. Delneri D, Hoyle DC, Gkargkas K, Cross EJM, Rash B, Zeef L, et al. Identification and
747 characterization of high-flux-control genes of yeast through competition analyses in
748 continuous cultures. Nat Genet. 2008;40(1):113–7.

749 63. Takemata N, Ohta K. Role of non-coding RNA transcription around gene regulatory
750 elements in transcription factor recruitment. RNA Biol. 2017;14(1):1–5.

751 64. Hooks KB, Naseeb S, Parker S, Griffiths-Jones S, Delneri D. Novel intronic RNA
752 structures contribute to maintenance of phenotype in *Saccharomyces cerevisiae.*
753 Genetics. 2016;203(3):1469–81.

754 65. Martens L, Rühle F, Stoll M. LncRNA secondary structure in the cardiovascular system.
755 Non-coding RNA Research. 2017;2:137–142.

66. Wang KC, Chang HY. Molecular Mechanisms of Long Noncoding RNAs. Mol Cell. 2011;43(6):904–14.

67. Parker S, Fraczek MG, Wu J, Shamsah S, Manousaki A, Dungrattanalert K, et al. A resource for functional profiling of noncoding RNA in the yeast *Saccharomyces cerevisiae*. RNA. 2017;23(8):1166–71

68. Wagih O, Usaj M, Baryshnikova A, VanderSluis B, Kuzmin E, Costanzo M, et al. SGAtools: one-stop analysis and visualization of array-based genetic interaction screens. Nucleic Acids Res. 2013;41:W591-W596.

69. Naseeb S, Delneri D. Impact of Chromosomal Inversions on the Yeast DAL Cluster. PLoS One. 2012;7(8):e42022.

70. Dobin A, Davis CA, Schlesinger F, Drenkow J, Zaleski C, Jha S, et al. STAR: ultrafast universal RNA-seq aligner. Bioinformatics. 2013;29(1):15–21.

71. Love MI, Huber W, Anders S. Moderated estimation of fold change and dispersion for RNA-seq data with DESeq2. Genome Biol. 2014;15(12):550.

72. Balakrishnan R, Park J, Karra K, Hitz BC, Binkley G, Hong EL, et al. YeastMine--an integrated data warehouse for *Saccharomyces cerevisiae* data as a multipurpose tool-kit. Database (Oxford). 2012;2012:bar062.

73. Hulsen T, de Vlieg J, Alkema W. BioVenn - A web application for the comparison and visualization of biological lists using area-proportional Venn diagrams. BMC Genomics. 2008;9.

74. Larsson J (2019). eulerr: Area-Proportional Euler and Venn Diagrams with Ellipses. R package version 6.0.0, https://cran.r-project.org/package=eulerr.

Supporting information

S1 Dataset.

This file contains the solid fitness data of the 372 mutant strains tested in 23 different conditions. It contains a summary of the clusters and the p-value per strain per condition

S2 Dataset.

This file contains the RNA-seq data divided by mutant, containing the list of significant DE genes per mutant strain. Tables are divided by protein-coding genes and non-coding transcripts

S1 Fig. Solid fitness of heterozygous deletions of essential ncRNAs, SUT075 and snR30

Bar charts displays the colony size of *SUT075Δ* and *snR30Δ* deletion strains when growing in (A) YPD and (B) YPD supplemented with 10% ethanol.

S2 Fig. Gene ontology for biological process enriched in DE genes in common between snR30 and SUT075. Bar chart displaying the 20 first significantly enriched GO terms. The negative logarithm of the adjusted p-value (base 10) after Holm-Bonferroni correction is represented on the x-axis. The figure was created using the DE genes in common for SUT075 and snR30 deletion mutants. n=1836.

S3 Fig. Histogram of GO terms from DE genes in *CUT494/SUT530/SUT468Δ* strain. Representative GO terms for biological processes for up-regulated (red) and down- regulated (green) genes in the *CUT494/SUT530/SUT468Δ* strain. Holm-Bonferroni p-value cutoff < 0.05; y –axis displays GO terms, x-axis shows the p-value that was transformed to –log10. The figure was created using the DE genes. n=137.

S4 Fig. Validation of DE genes obtained during RNA-seq by qPCRs. Relative mRNA levels of (A) *PDR3* and (B) *YOX1* in *SUT035*Δ strain, (C) *PDC6* and (D) *PIL1* in *SUT125*Δ and the TFs (E) *PDR3*, (F) Y*OX1* and (G) *MOT3* in *SUT126*Δ strain analyzed by RT-qPCR. Relative mRNA levels were quantified by qPCR and compared by *t*-test.

S5 Fig. SUT125, SUT126 and SUT035 reveal an important role in mitochondrial processes. Gene Ontology of biological processes inferred from dysregulated coding targets in common in *SUT125*Δ, *SUT126*Δ and *SUT035*Δ deletion strains. Significantly first enriched GO terms for biological processes (Holm-Bonferroni adjusted p-value <0.05) are listed on the y-axis, and the negative log of the adjusted p-value (base 10) is represented on the x-axis. The figure was created using the DE genes in common for SUT125, SUT126 and SUT035 n=481.

S6 Fig. Gene Ontology of biological processes inferred from DE protein coding genes in S*UT532Δ* deletion mutant strain. Significantly enriched representative GO terms for biological processes for up-regulated (red, n=172) and down-regulated (green, n=236) in *SUT532Δ* deletion strain. P-value was calculated using Holm-Bonferroni correction. Representative GO terms are listed on the y-axis, and the negative log of the adjusted p-value (base 10) is represented on the x-axis.

S7 Fig. Area proportional Venn diagram of DE transcripts between cluster 1, 2 and 5. Number of (A) Protein coding genes (96) and (B) Non-coding transcripts (15) in common dysregulated among deletion strains in cluster 1 (*SUT125Δ, SUT035Δ*), 2 (*SUT126Δ*) and 5 (*SUT532Δ*). Venn diagram generated using Eulerr [74]

S8 Fig. Venn diagram representing TFs in common between phenotypic related ncRNA deletion mutants with significant impact on the genome. Area proportional Venn diagram generated by BioVenn [73] using the number of TFs dysregulated in deletion strains in cluster 1 (*SUT125*Δ, *SUT035*Δ) and 2 (*SUT126*Δ). The overlapping (23 TFs) is shown in a dark green colour.

836 **S9 Fig. Altered expression levels of target genes in ncRNA deletion mutant strains are**
837 **independent of *kanMX* marker.** Relative mRNA levels of the transcriptional repressor (A)
838 *YOX1* and the transcriptional activator (B) *PDR3* in *SUT125*Δ and *SUT126*Δ deletion mutant
839 strains with and without *kanMX.* The *kanMX* cassette does not influence genes located
840 distantly from the SUT disruption. Relative mRNA levels were quantified by qPCR and
841 compared by *t*-test.

842

843 **S1 Table.** Characteristic parameters of growth curves of deletion mutant strains assessed in
844 liquid media. Tables show mean values normalized with wild type, standard deviation (SD),
845 adjusted p-value and significance per parameter.

846 **S2 Table**. List of transcription factors DE in mutant strains.

847 **S3 Table.** List of yeast strains and plasmids used in this study

848 **S4 Table.** List of primers for Quantitative real time PCR (qPCR) used in this study

849 **S5 Table**. List of media condition used for solid fitness analysis for the haploid ncRNA deletion
850 collection.

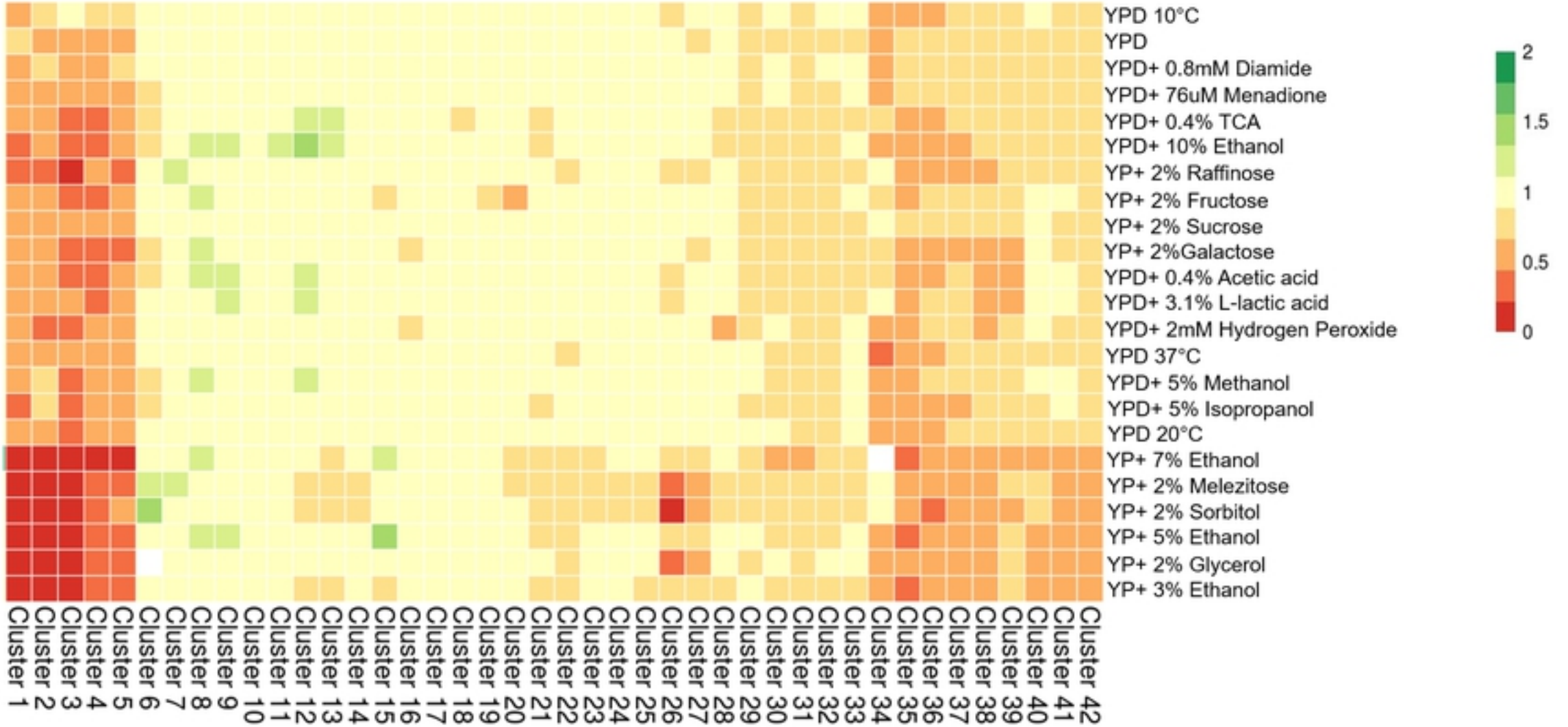
YPD 10°C
YPD
YPD+ 0.8mM Diamide
YPD+ 76uM Menadione
YPD+ 0.4% TCA
YPD+ 10% Ethanol
YP+ 2% Raffinose
YP+ 2% Fructose
YP+ 2% Sucrose
YP+ 2%Galactose
YPD+ 0.4% Acetic acid
YPD+ 3.1% L-lactic acid
YPD+ 2mM Hydrogen Peroxide
YPD 37°C
YPD+ 5% Methanol
YPD+ 5% Isopropanol
YPD 20°C
YP+ 7% Ethanol
YP+ 2% Melezitose
YP+ 2% Sorbitol
YP+ 5% Ethanol
YP+ 2% Glycerol
YP+ 3% Ethanol
2
1.5
1
0.5
0
Cluster 1
Cluster 2
Cluster 3
Cluster 4
Cluster 5
Cluster 6
Cluster 7
Cluster 8
Cluster 9
Cluster 10
Cluster 11
Cluster 12
Cluster 13
Cluster 14
Cluster 15
Cluster 16
Cluster 17
Cluster 18
Cluster 19
Cluster 20
Cluster 21
Cluster 22
Cluster 23
Cluster 24
Cluster 25
Cluster 26
Cluster 27
Cluster 28
Cluster 29
Cluster 30
Cluster 31
Cluster 32
Cluster 33
Cluster 34
Cluster 35
Cluster 36
Cluster 37
Cluster 38
Cluster 39
Cluster 40
Cluster 41
Cluster 42

Figure 1

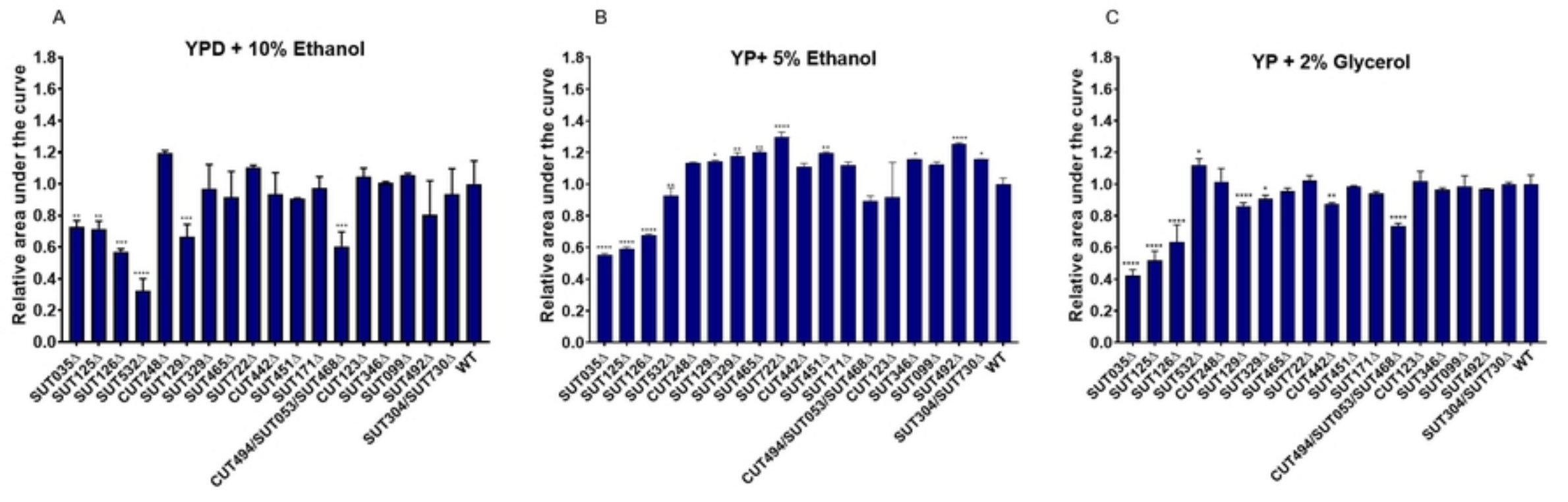
A
YPD + 10% Ethanol
Relative area under the curve
B
YP+ 5% Ethanol
Relative area under the curve
C
YP + 2% Glycerol
Relative area under the curve
SUT035Δ
SUT125Δ
SUT126Δ
SUT532Δ
CUT248Δ
SUT129Δ
SUT329Δ
SUT465Δ
SUT722Δ
CUT442Δ
SUT451Δ
SUT171Δ
CUT494/SUT053/SUT468Δ
CUT123Δ
SUT346Δ
SUT099Δ
SUT492Δ
SUT304/SUT730Δ
WT

Figure 2

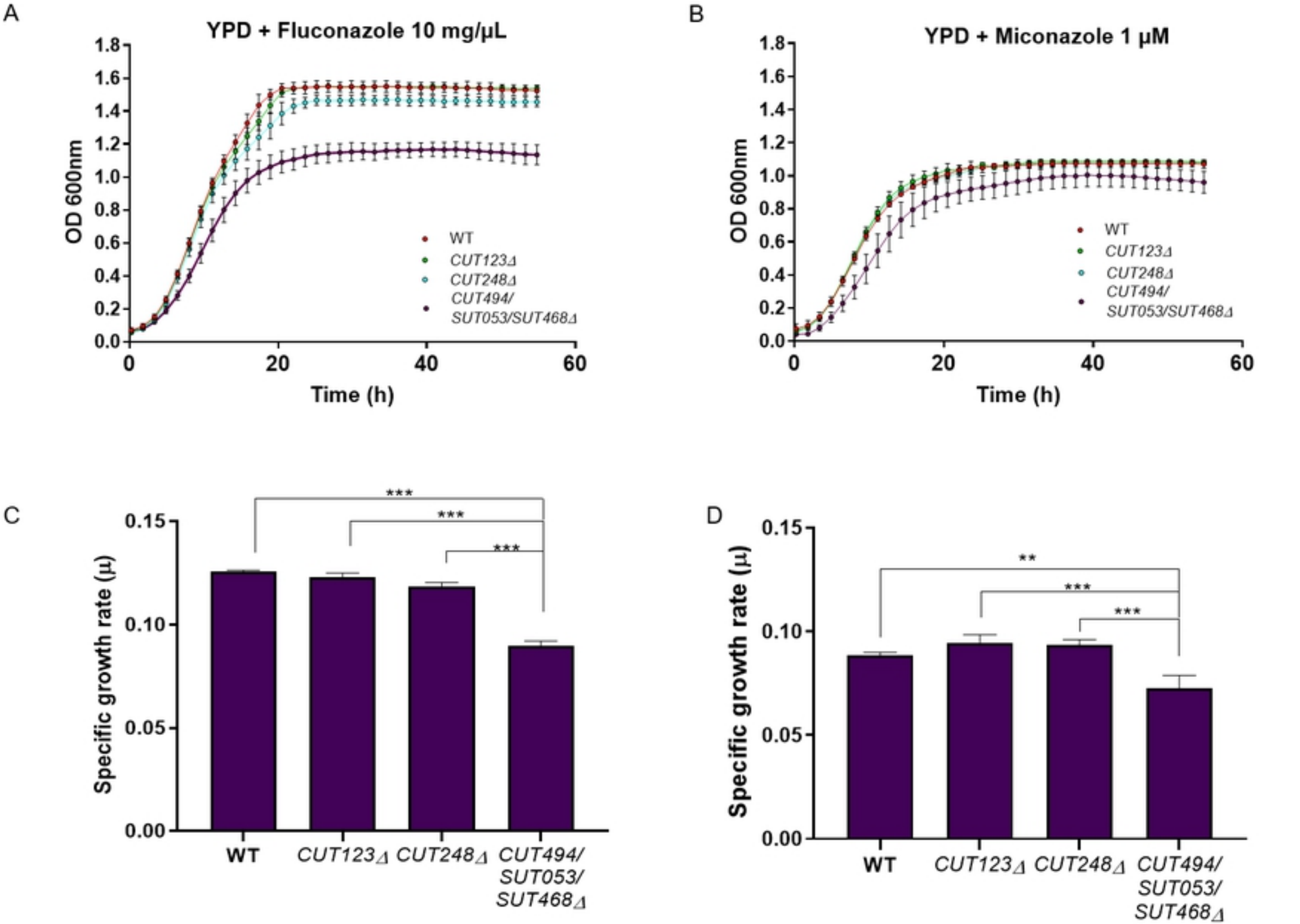
A
YPD + Fluconazole 10 mg/µL
OD 600nm
Time (h)
WT
CUT123Δ
CUT248Δ
CUT494/
SUT053/SUT468Δ
B
YPD + Miconazole 1 µM
OD 600nm
Time (h)
WT
CUT123Δ
CUT248Δ
CUT494/
SUT053/SUT468Δ
C
Specific growth rate (µ)
***
***
***
WT
CUT123Δ
CUT248Δ
CUT494/
SUT053/
SUT468Δ
D
Specific growth rate (µ)
**
***
***
WT
CUT123Δ
CUT248Δ
CUT494/
SUT053/
SUT468Δ

Figure 3

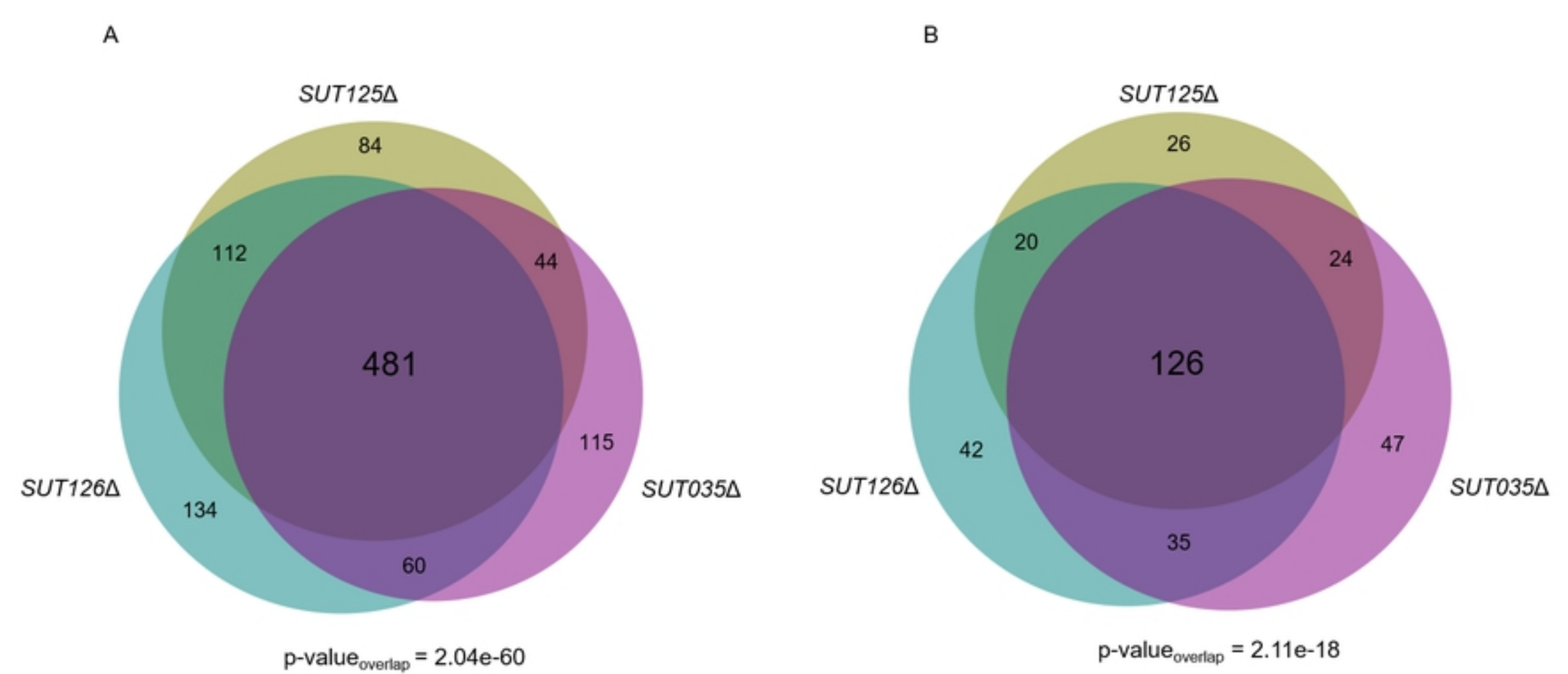
A
SUT125Δ
84
112
44
481
115
SUT126Δ
134
60
SUT035Δ
p-value$_{overlap}$ = 2.04e-60
B
SUT125Δ
26
20
24
126
42
47
SUT126Δ
35
SUT035Δ
p-value$_{overlap}$ = 2.11e-18

Figure 4

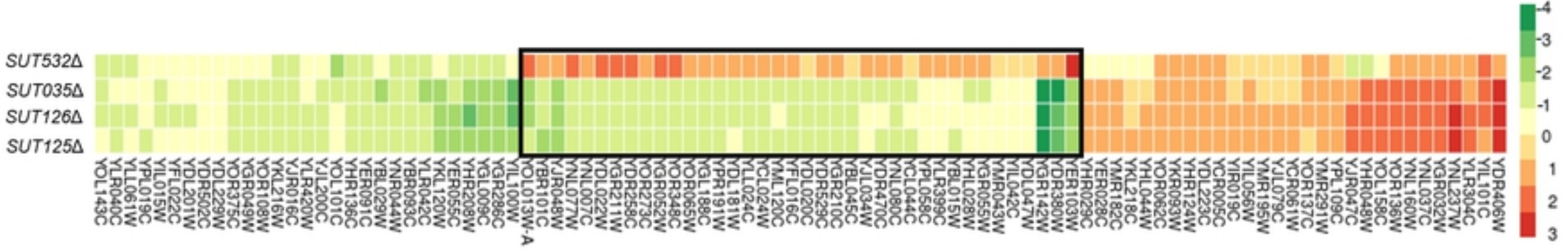
SUT532Δ
SUT035Δ
SUT126Δ
SUT125Δ
YOL143C
YLR040C
YLL061W
YPL019C
YIL015W
YFL022C
YDL201W
YDR502C
YDL229W
YOR375C
YGR049W
YOR108W
YKL216W
YJR016C
YLR420W
YJL200C
YOL101C
YER091C
YHR136C
YBL029W
YNR044W
YBR093C
YLR042C
YKL120W
YER055C
YHR208W
YGL009C
YGR286C
YIL100W
YOL013W-A
YBR101C
YJR048W
YNL077W
YNL007C
YDL022W
YGR211W
YDR258C
YOR273C
YGR052W
YOR348C
YOR065W
YGL188C
YPR191W
YDL181W
YDL024C
YCL024W
YML120C
YFL016C
YDL020C
YDR529C
YGR210C
YBL045C
YJL034W
YDR470C
YNL080C
YCL044C
YPL058C
YLR399C
YBL015W
YHL028W
YGR055W
YMR043W
YIL042C
YDL047W
YGR142W
YDR380W
YER103W
YHR029C
YER028C
YMR182C
YKL218C
YHL044W
YOR062C
YKR093W
YHR124W
YDL223C
YCR005C
YIR019C
YIL056W
YMR195W
YJL079C
YCR061W
YOR137C
YMR291W
YPL109C
YJR047C
YHR048W
YOL158C
YOR136W
YNL160W
YNL037C
YGR032W
YNL237W
YLR304C
YIL101C
YDR406W
4
3
2
1
0
1
2
3

Figure 5

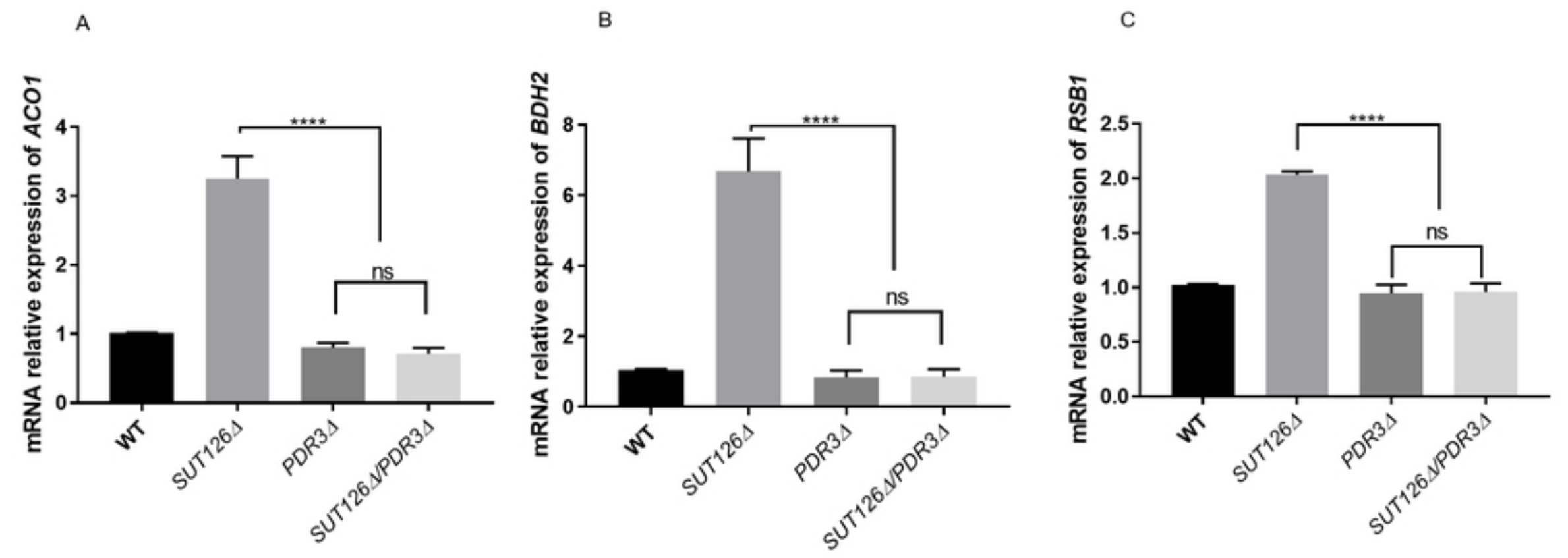
A
mRNA relative expression of ACO1
4
3
2
1
0
****
ns
WT
SUT126Δ
PDR3Δ
SUT126Δ/PDR3Δ
B
mRNA relative expression of BDH2
8
6
4
2
0
****
ns
WT
SUT126Δ
PDR3Δ
SUT126Δ/PDR3Δ
C
mRNA relative expression of RSB1
2.5
2.0
1.5
1.0
0.5
0.0
****
ns
WT
SUT126Δ
PDR3Δ
SUT126Δ/PDR3Δ

Figure 6

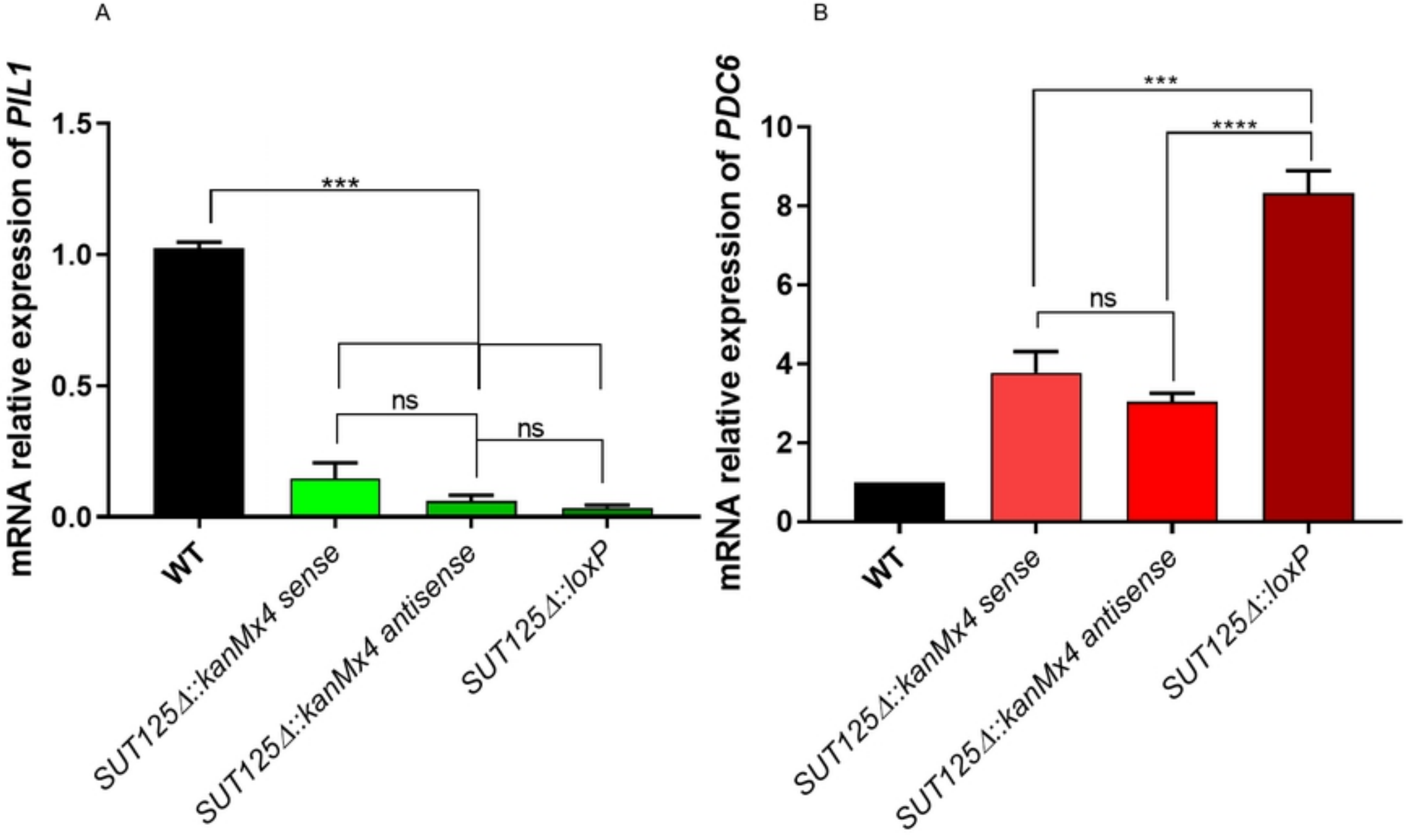
A
mRNA relative expression of PIL1
1.5
1.0
0.5
0.0
***
ns
ns
WT
SUT125Δ::kanMx4 sense
SUT125Δ::kanMx4 antisense
SUT125Δ::loxP
B
mRNA relative expression of PDC6
10
8
6
4
2
0
***
****
ns
WT
SUT125Δ::kanMx4 sense
SUT125Δ::kanMx4 antisense
SUT125Δ::loxP

Figure 7

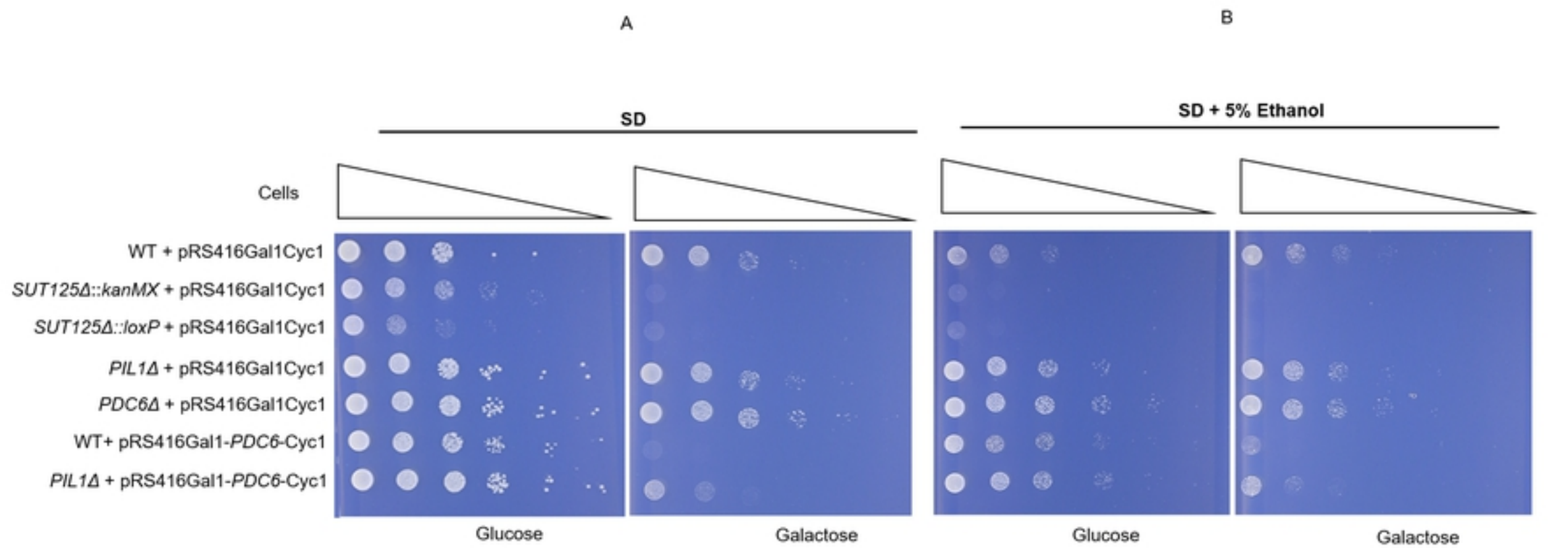
A
B
SD
SD + 5% Ethanol
Cells
WT + pRS416Gal1Cyc1
SUT125Δ::kanMX + pRS416Gal1Cyc1
SUT125Δ::loxP + pRS416Gal1Cyc1
PIL1Δ + pRS416Gal1Cyc1
PDC6Δ + pRS416Gal1Cyc1
WT+ pRS416Gal1-PDC6-Cyc1
PIL1Δ + pRS416Gal1-PDC6-Cyc1
Glucose
Galactose
Glucose
Galactose

Figure 8

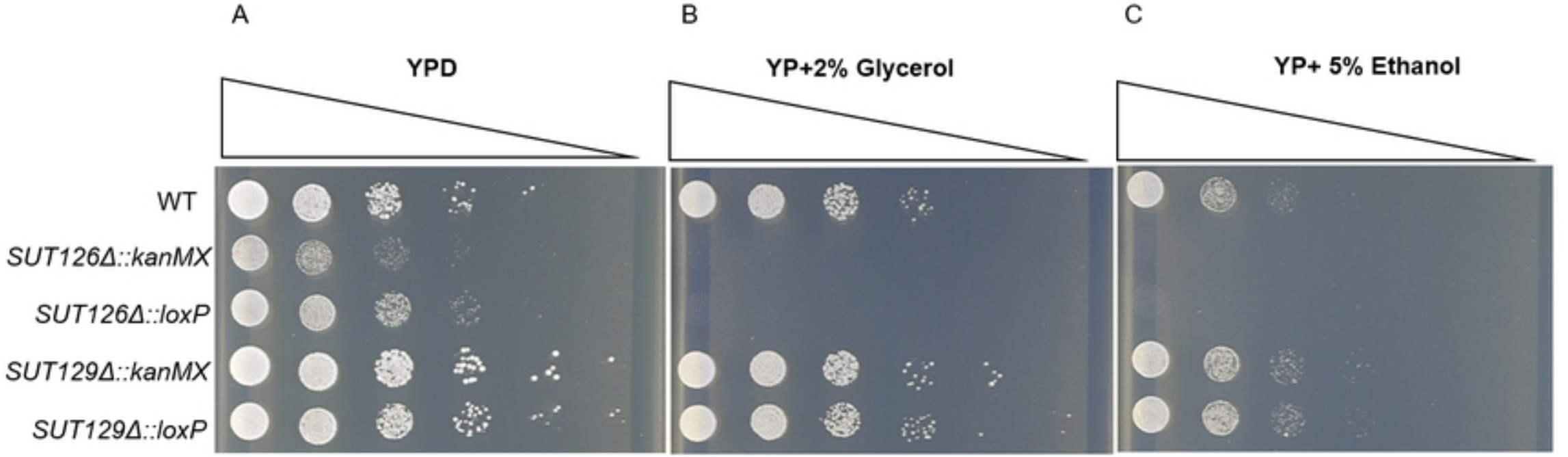
A
YPD
B
YP+2% Glycerol
C
YP+ 5% Ethanol
WT
SUT126Δ::kanMX
SUT126Δ::loxP
SUT129Δ::kanMX
SUT129Δ::loxP

Figure 9

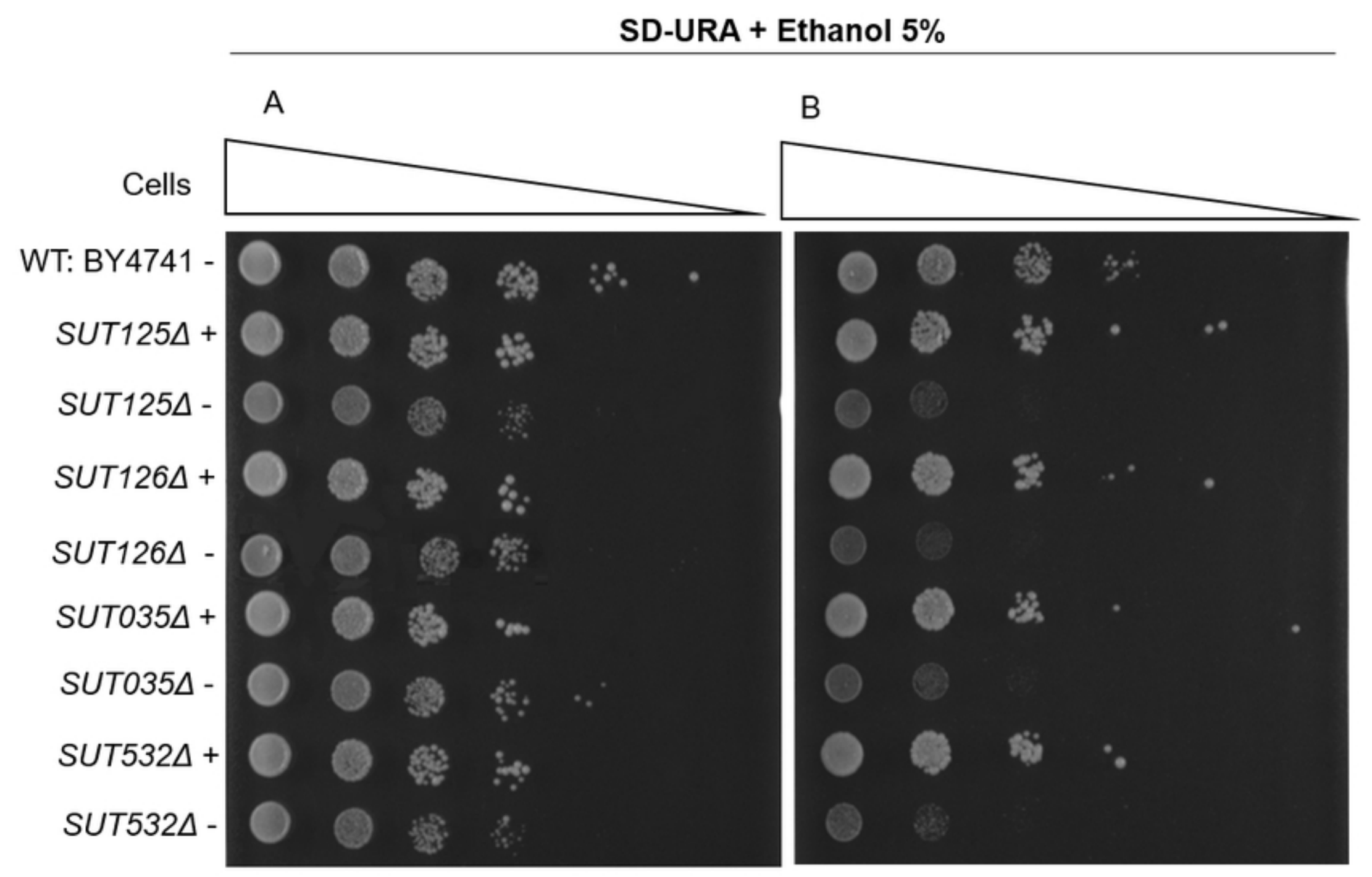
SD-URA + Ethanol 5%
A
B
Cells
WT: BY4741 -
SUT125Δ +
SUT125Δ -
SUT126Δ +
SUT126Δ -
SUT035Δ +
SUT035Δ -
SUT532Δ +
SUT532Δ -

Figure 10